Regulatory Interdependence of Cloned Epithelial Na^+ Channels and P2X Receptors

Scott S. Wildman,* Joanne Marks,* Linda J. Churchill,* Claire M. Peppiatt,† Ahmed Chraibi,‡ David G. Shirley,* Jean-Daniel Horisberger,§ Brian F. King,* and Robert J. Unwin*

**Department of Physiology and Centre for Nephrology, Royal Free and University College Medical School, University College London, London, United Kingdom; †Department of Physiology, University College London, London, United Kingdom; ‡Faculté de Medecine, Department de Physiologie et Biophysique, Université de Sherbrooke, Sherbrooke, Québec, Canada; and §Institut de Pharmacologie et de Toxicologie, Université de Lausanne, Lausanne, Switzerland*

Epithelial Na^+ channels (ENaC) coexist with a family of ATP-gated ion channels known as P2X receptors in the renal collecting duct. Although ENaC is itself insensitive to extracellular ATP, tubular perfusion of ATP can modify the activity of ENaC. To investigate a possible regulatory relationship between P2X receptors and ENaC, coexpression studies were performed in *Xenopus* oocytes. ENaC generated a persistent inward Na^+ current that was sensitive to the channel blocker amiloride ($I_{am\text{-}s}$). Exogenous ATP transiently activated all cloned isoforms of P2X receptors, which in some cases irreversibly inhibited $I_{am\text{-}s}$. The degree of inhibition depended on the P2X receptor subtype present. Activation of $P2X_2$, $P2X_{2/6}$, $P2X_4$, and $P2X_{4/6}$ receptor subtypes inhibited $I_{am\text{-}s}$, whereas activation of $P2X_1$, $P2X_3$, and $P2X_5$ receptors had no significant effect. The degree of inhibition of $I_{am\text{-}s}$ correlated positively with the amount of ionic charge conducted by P2X receptor subtypes. ENaC inhibition required Na^+ influx through $I_{am\text{-}s}$-inhibiting P2X ion channels but also Ca^{2+} influx through $P2X_4$ and $P2X_{4/6}$ ion channels. P2X-mediated inhibition of $I_{am\text{-}s}$ was found to be due to retrieval of ENaC from the plasma membrane. Maximum amplitudes of ATP-evoked P2X-mediated currents (I_{ATP}) were significantly increased for $P2X_2$, $P2X_{2/6}$, and $P2X_5$ receptor subtypes after coexpression of ENaC. The increase in I_{ATP} was due to increased levels of plasma membrane–bound P2X receptor protein, suggesting that ENaC modulates protein trafficking. In summary, ENaC was downregulated by the activation of $P2X_2$, $P2X_{2/6}$, $P2X_4$, and $P2X_{4/6}$ receptors. Conversely, ENaC increased the plasma membrane expression of $P2X_2$, $P2X_{2/6}$, and $P2X_5$ receptors.

J Am Soc Nephrol 16: 2586–2597, 2005. doi: 10.1681/ASN.2005020130

The amiloride-sensitive epithelial sodium channel (ENaC) largely determines the extent of Na^+ reabsorption from tubular fluid along the distal nephron and consequently is crucial for the maintenance of whole-body Na^+ balance and regulation of extracellular fluid volume (1). The physiologic importance of ENaC is exemplified by several inheritable human mutations of the genes encoding ENaC subunits that lead to abnormal Na^+ balance and altered BP (2). There has been rapid progress in understanding the regulation of ENaC activity since the constituent subunits were cloned (3). ENaC is composed of three nonidentical but homologous subunits (α, β, and γ) that form a tetrameric structure with a stoichiometry of two α-, one β-, and one γ-subunit(s) (4). Expression of these ENaC subunits in *Xenopus laevis* oocytes results in a persistent Na^+ conductance pathway that corresponds to the biophysical and pharmacologic properties of native epithelial Na^+ channels present on the apical membrane of the collecting duct (CD) (4).

It is well documented that several hormones can regulate ENaC activity (most notably, aldosterone and vasopressin). In addition, since the advent of cloning and expression studies, it has been demonstrated that ENaC is regulated by a number of intracellular signaling pathways activated by intra- and extracellular factors (*e.g.*, Na^+ itself, free Ca^{2+}, Cl^-, H^+), second messengers (cAMP and protein kinases), and regulatory proteins (G proteins, Nedd4, certain proteases, and actin filaments) (4–6). These signals control ENaC activity *via* a number of diverse mechanisms, including changes in the kinetics of channel opening and closing, channel synthesis, regulation of intracellular channel trafficking to the plasma membrane, membrane insertion, and channel endocytosis (7). It is interesting that a number of factors that are known to regulate ENaC activity—such as changes in intracellular cations, changes in cAMP levels, and the activation of regulatory G proteins—can be modulated by nucleotide receptors (P2 receptors) (8).

There are two classes of P2 receptors: P2X and P2Y (8). The P2X class consists of seven cloned subunits, which form seven trimeric nucleotide-gated homomeric ion channels ($P2X_{1\text{ to }7}$) and five established heteromeric ion-channel assemblies

Received February 2, 2005. Accepted May 30, 2005.

Published online ahead of print. Publication date available at www.jasn.org.

Address correspondence to: Dr. Scott S. Wildman, Department of Physiology and Centre for Nephrology, Royal Free and University College Medical School, University College London, Rowland Hill Street, London NW3 2PF, UK. Phone: +44-0-207-794-0500 ext. 5204; Fax: +44-0-207-472-6476; E-mail: s.wildman@medsch.ucl.ac.uk

ISSN: 1046-6673/1609-2586

($P2X_{1/2,1/5,2/3,2/6,4/6}$). P2X receptors are permeable to Na^+, K^+, Ca^{2+}, and, in some cases, Cl^- and on activation cause cell depolarization (9–12). The P2Y class consists of eight G protein–coupled nucleotide-activated receptors ($P2Y_{1,2,4,6,11\ to\ 14}$), which can mobilize intracellular Ca^{2+}, alter intracellular cAMP levels, or release their regulatory $\beta\gamma$ subunits (8). Both P2X and P2Y receptor subtypes are expressed in the nephron (13), and both the variety and the abundance of P2X receptors are highest in the distal nephron. Multiple P2X receptors ($P2X_1$ to $P2X_7$) have been molecularly identified in cell models of the distal nephron (14,15), and our own studies in native rat tissue have immunolocalized $P2X_4$, $P2X_5$, and $P2X_6$ receptor subunits to the distal tubule and CD principal cells (16), where they may co-localize with ENaC in the apical membrane.

Extracellular ATP can modify ENaC activity, although ENaC itself is insensitive to extracellular ATP (17). Consequently, it has been proposed that ATP must act indirectly to regulate ENaC by activating cell surface P2 receptors (16,18). This theory has been supported by a number of studies demonstrating P2 receptor–mediated inhibition of sodium reabsorption in native CD epithelia (19,20) and renal epithelial cell lines (14,21,22). ATP-evoked inhibition of Na^+ reabsorption in the distal nephron is usually thought to be the consequence of stimulation of P2Y receptors (23). However, two separate studies have inferred that apical P2X receptors may mediate ENaC inhibition. First, a study on mIMCD-K2 cells (an immortalized CD cell line) described inhibition of Na^+ absorption (and stimulation of Cl^- secretion) after activation of $P2X_3$ and $P2X_4$ receptors (14). Second, we have proposed P2X receptor–mediated inhibition of ENaC in an *in vivo* microperfusion study of the rat CD, in which $^{22}Na^+$ recovery was measured to assess Na^+ reabsorption after P2 receptor activation (19). We showed that a nonhydrolyzable analogue of ATP, ATPγS, inhibited Na^+ reabsorption in Na^+-restricted animals, whereas other nonhydrolyzable analogues had no measurable effect on $^{22}Na^+$ uptake. Investigations into the selectivity and the potency of this series of analogues on recombinant P2 receptors corresponding to those found in the rat CD, expressed in *Xenopus* oocytes, suggested that $P2X_{4/6}$ receptors mediated the inhibition of Na^+ reabsorption (24).

Furthermore, it has been demonstrated that ENaC can stimulate an increase in the surface expression of certain ion channels in the kidney, namely cystic fibrosis transmembrane conductance regulator (CFTR) chloride channels and ROMK1 potassium channels (25). Thus, the possibility exists that ENaC may also increase expression levels of P2X receptors.

The molecular mechanisms by which P2X receptors may regulate ENaC activity and, conversely, the mechanisms by which ENaC might influence P2X receptor activity are unknown. These issues have been addressed in the present study by performing coexpression experiments in the *Xenopus laevis* oocyte recombinant model, using two-electrode voltage-clamp recordings in combination with measurements of surface expression of ENaC and P2X ion channels.

Materials and Methods

Oocyte Preparation

Xenopus laevis frogs were anesthetized in tricaine (0.4% wt/vol) and killed by decapitation, and their ovarian lobes were removed surgically. Stage V and VI oocytes were defolliculated by a two-step process involving collagenase treatment (type IA, 1.5 mg/ml in a Ca^{2+}-free Ringer solution, for 2 h) followed by mechanical stripping away of the follicular layer by fine forceps. Defolliculated oocytes were injected with 50 nl of a cRNA/sterile water mixture or cRNA/cRNA combination (50%/50%) in the case of heteromeric assemblies (total cRNA quantities: rat α-, β-, γ-ENaC, 10 ng of each subunit; rat $P2X_1$, $P2X_3$, $P2X_4$, $P2X_5$, $P2X_6$, 50 ng; rat $P2X_2$, 20 ng; rat $P2X_{2/6}$ and rat $P2X_{4/6}$, 50 ng of each subunit). Injected oocytes were incubated for 24 h at 18°C in a low-Na^+ modified Barth's solution that contained (in mM) 1 NaCl, 60 *N*-methyl-D-glutamine-Cl (NMDG), 40 KCl, 0.8 $MgSO_4$, 0.3 $Ca(NO_3)_2$, 0.4 $CaCl_2$, and 10 HEPES-NMDG (pH 7.4) and was supplemented with 50 μg/L gentamicin sulfate, then kept at 4°C for up to 5 d until used in electrophysiologic experiments. All experiments conformed to local and British Home Office regulations with regard to the Animal Scientific Procedures Act (1986).

Two-Electrode Voltage Clamp

Oocytes were studied using the two-electrode voltage-clamp technique. Oocytes were clamped at a holding potential (V_h) of −100 mV, with two exceptions: (*1*) In initial experiments to determine the IC_{50} value for amiloride (the concentration of amiloride that blocked ENaC-mediated currents by 50%), in which the V_h was clamped at −10 mV in the absence of amiloride (20 min), to avoid channel rundown, and −100 mV while recording in the presence of amiloride (40 s; Figure 1A); and (*2*) in experiments to determine the effects of changing cytosolic Cl^- levels on P2X-mediated inhibition of amiloride-sensitive currents ($I_{am\text{-}s}$; by incubating oocytes in low extracellular Cl^- Ringer solution supplemented with 10 μM amiloride [low $[Cl^-]_{int}$] for 72 h), in which the V_h was clamped at −30 mV because of the poor health of the oocytes. The voltage-recording and current-recording microelectrodes (1 to 5 MΩ tip resistance) were filled with 3.0 M KCl. Oocytes were superfused with a Ringer solution (10 ml/min, 18°C) that contained (in mM) 100 NaCl, 3.0 KCl, 10 HEPES, and 1.8 $CaCl_2$ (pH 7.4), by a gravity-fed continuous flow system that allowed rapid drug addition and washout. In ion-substitution experiments, Na^+, Cl^-, or Ca^{2+} concentrations of the Ringer solution were altered as stated in the text and in Table 1. The $I_{am\text{-}s}$ was determined by subtracting the value measured in the absence of 10 μM amiloride (90 s) from that measured in the presence of amiloride in the bathing Ringer solution, with a rest time of 20 min after each removal of amiloride. ATP-activated currents (I_{ATP}) were recorded after addition of agonist for 90 s or until the current reached a peak, then washed for a period of 20 min for all of the P2X receptors tested. Electrophysiologic data were stored on a computer using an MP100 WSW interface (Biopac Systems, Goleta, CA) and analyzed (including area-under-the-curve calculations) using the software package Acqknowledge III (Biopac Systems).

Detection of Cell Surface Expression by Chemiluminescence

For binding experiments, α, β, and γ rat ENaC subunits were tagged, as described by Firsov *et al.* (26), with the FLAG reporter octapeptide (FLAG sequence: DYKDDDDK; D, aspartate; Y, tyrosine; K, lysine) in the extracellular loop directly above the COOH-terminal of the second transmembrane segment of each subunit. Oocytes were incubated for 30 min in Ringer solution supplemented with 1% BSA at 4°C to block nonspecific binding of the antibodies. Subsequently, oocytes were incubated for 45 min at 4°C with 2 μg/ml mouse anti-FLAG (M2)

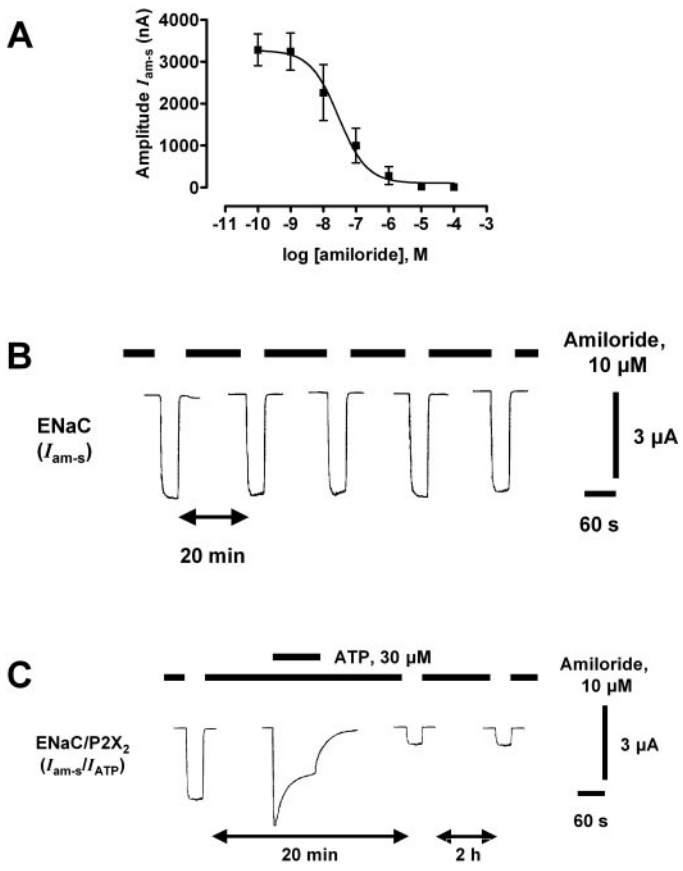

Figure 1. Amiloride-sensitive epithelial Na^+ channel (ENaC)-mediated currents are inhibited by the activation of ATP-gated $P2X_2$ receptors. (A) Inhibition curve for amiloride blockade of ENaC-mediated currents in oocytes that expressed ENaC ($n = 3$). (B) Typical trace showing consistent ENaC-mediated amiloride-sensitive currents (I_{am-s}) evoked by the removal of IC_{100} concentration of amiloride (10 μM). Oocytes were voltage clamped at −100 mV (holding potential [V_h]), and 20 min was left between evoked currents. (C) A typical trace showing an oocyte coexpressing ENaC and $P2X_2$ receptors, in which application of ATP (30 μM) for 120 s in the presence of amiloride (10 μM) evokes a $P2X_2$-mediated current (ATP-activated current [I_{ATP}]). Subsequent removal of amiloride results in an inhibition of ENaC-mediated currents (I_{am-s}), irreversible over a 2-h period.

peroxidase (horseradish peroxidase) conjugated antibody (Sigma-Aldrich, St. Louis, MO) in 1% BSA/Ringer. Oocytes then were washed, initially in 1% BSA/Ringer (45 min at 4°C), then in Ringer solution without BSA (45 min at 4°C). Individual oocytes were placed in 200 μl of Visualizer Western Blot Detection solution (Upstate Cell Signaling Solutions, Dundee, UK) for 10 s, and chemiluminescence was quantified using a Fluor-S Multiimager (Bio-Rad, Hemel Hempstead, UK) by integrating the signal over a period of 30 s. Results are given in relative light units (RLU) as a function of measured density of chemiluminescence after the correction for background chemiluminescence. Nonspecific binding was determined from parallel assays of noninjected oocytes.

Western Blot Analysis

Oocytes were homogenized (25 oocytes per experimental group) in buffer that contained (in mM) 10 HEPES, 1 EDTA, 0.5 PMSF (pH 7.4), and 6.25×10^3 IU/L Aprotinin, using an Ultra Turrax homogenizer (Janke & Kunkel, Staufen, Germany) at half speed for 20 s. Homogenates were centrifuged for 10 min at 3000 rpm and the supernatant was re-centrifuged at 13,000 rpm for 30 min. The pellet was resuspended in buffer, and high-speed centrifugation was repeated. The resulting pellet was resuspended in 25 μl of buffer, and the final protein concentration was determined using the Bradford method (27). All steps were performed at 4°C.

Oocyte membrane preparations (15 μg of protein) were then solubilized in Laemmli sample buffer that contained 2% (wt/vol) SDS and 3% (wt/vol) dithiothreitol and electrophoresed on a 10% SDS polyacrylamide gel using 25 mM Tris, 192 mM glycine, and 0.1% (wt/vol) SDS running buffer (pH 8.3) at 20 mA per gel. The proteins were transferred to nitrocellulose membranes by electrophoretic blotting for 1 h at a constant current of 1 mA/cm^2 (Transblot semidry transfer cell; Bio-Rad) using transfer buffer that contained 10% (vol/vol) methanol, 25 mM Tris, 192 mM glycine, and 0.1% (wt/vol) SDS (pH 8.2 to 8.4). Nonspecific protein-binding sites were then blocked with PBS-T (pH 7.4) that contained 0.1% Tween 20 and 6% (wt/vol) fat-free milk powder for 1 h at room temperature. The membranes were incubated with rabbit anti-rat $P2X_2$ antibody (Alomone, Jerusalem, Israel) at 1:1000 in PBS-T for 16 h at 4°C. The membranes were then washed with PBS-T and incubated with a swine anti-rabbit IgG antibody conjugated to horseradish peroxidase (1:2000 dilution; Amersham Biosciences, Piscataway, NJ) for 1 h at room temperature and finally washed again with PBS-T (2 × 15 min). Bound antibodies were detected using a Visualizer Western Blot Detection Kit (Upstate Cell Signaling Solutions) and visualized and quantified (for 30 s) using a Fluor-S Multiimager (Bio-Rad). Band density was expressed in arbitrary units. All Western blot experiments were repeated using four different batches of oocytes.

Statistical Analyses

All data are presented as mean values ± SEM; n indicates the number of oocytes from different frogs; significance was evaluated by t test (Instat v2.05a; GraphPad Software, San Diego, CA) with $P < 0.05$ considered significant.

Results

ENaC and P2X Receptor Coexpression

Heterotetrameric ENaC expressed in defolliculated oocytes carried a persistent inward Na^+ current that was amiloride sensitive (I_{am-s}). Amiloride (100 pM to 10 μM) concentration-dependently blocked I_{am-s} with an IC_{50} value of 29.0 ± 14.9 nM ($n = 3$) at −100 mV, and full blockade occurred at ≤10 μM (Figure 1A). The effect of amiloride was rapidly reversed on washout. To avoid ENaC rundown in response to cytosolic Na^+ accumulation, oocytes were used in all further experiments with 10 μM amiloride present. Brief removal of amiloride blockade (40 s) at 20-min intervals resulted in large (≥3 μA) reproducible I_{am-s} (Figure 1B).

ENaC was coexpressed with P2X receptors to investigate whether activation of P2X receptors by extracellular ATP had an effect on I_{am-s}. Figure 1C shows a typical trace in which ENaC was coexpressed with homotrimeric ATP-gated $P2X_2$ receptors. Activation of the $P2X_2$ receptor by ATP (30 μM, approximately EC_{80}) elicited a large (approximately 4 μA), slowly desensitizing, inward cationic membrane current (I_{ATP}) in the presence of 10 μM amiloride. Activation of the $P2X_2$ receptor 5 min before the removal of amiloride resulted in an approximately 80% decrease in the amplitude of I_{am-s}. The

Table 1. Solutions used for oocyte current measurements

	Test Solution (Ringer; mM)	Low Na^+ Ringer (mM)	Low Cl^- Ringer (mM)	Zero Ca^{2+} Ringer (mM)
NaCl	100	80	—	100
KCl	3.0	3.0	3.0	3.0
HEPES	10	10	10	10
$CaCl_2$	1.8	1.8	1.8	—
$NMDG^+$	—	20	—	—
$BaCl_2$	—	5	—	1.8
TEA-Cl	—	10	—	—
EGTA	—	—	—	1.0
Na-gluconate	—	—	100	—
pH	7.4 (NaOH)	7.4 (NaOH)	7.4 (NaOH)	7.4 (NaOH)

inhibition in $I_{am\text{-}s}$ after $P2X_2$ receptor activation did not change over a period of 2 h and therefore was considered irreversible. When expressed alone, ENaC was found to be insensitive to extracellular ATP (100 μM; maximal $I_{am\text{-}s}$ values pre- and post-ATP challenge were 3428 ± 511 and 3354 ± 543 nA, respectively), and all P2X receptors were found to be insensitive to extracellular amiloride (10 μM).

P2X-Mediated Inhibition of $I_{am\text{-}s}$

Homomeric and heteromeric P2X receptors were coexpressed with ENaC and tested for their ability to inhibit $I_{am\text{-}s}$. Activation of homomeric $P2X_2$ and $P2X_4$ receptors (by 100 and 30 μM ATP, respectively) resulted in a significant inhibition of $I_{am\text{-}s}$ (by 80 ± 6%, $n = 3$, $P < 0.01$ and 52 ± 5%, $n = 3$, $P < 0.01$; respectively; Figure 2A). Previously characterized (pharmacologically and biophysically) heteromeric P2X receptor assemblies $P2X_{2/6}$ and $P2X_{4/6}$ (9), when activated by 100 μM ATP, also significantly inhibited $I_{am\text{-}s}$ (by 72 ± 3%, $n = 3$, $P < 0.01$ and 45 ± 2%, $n = 3$, $P < 0.01$; respectively; Figure 2A). In contrast, activation of coexpressed $P2X_1$, $P2X_3$, $P2X_5$, and $P2X_6$ receptors had no significant effect on the amplitude of $I_{am\text{-}s}$. The rank order of relative efficacy of P2X receptors (activated by an EC_{100} concentration of ATP) to inhibit $I_{am\text{-}s}$ was $P2X_2 \geq P2X_{2/6} > P2X_4 = P2X_{4/6}$.

P2X receptor subtypes present strikingly different activation and inactivation properties (9). Homomeric and heteromeric assemblies of $P2X_1$ and $P2X_3$ receptors are defined as rapidly inactivating, $P2X_5$ and $P2X_6$ homomeric assemblies as poorly activating, and homomeric and heteromeric $P2X_2$ and $P2X_4$ assemblies as slowly inactivating (Figure 2B). During electrophysiologic recordings, it became clear that only the slowly inactivating receptor subtypes ($P2X_2$, $P2X_4$, $P2X_{2/6}$, and $P2X_{4/6}$) that also mediated the largest amplitude currents resulted in the inhibition of $I_{am\text{-}s}$. Therefore, we investigated the correlation between $I_{am\text{-}s}$ inhibition and the size of I_{ATP} for these receptor subtypes. For a range of ATP concentrations (100 nM to 100 μM; one concentration per cell repeated on at least three cells), a linear relationship was found between the area under the curve ($I \times t = Q$, or charge transfer) of I_{ATP} and the percentage inhibition of $I_{am\text{-}s}$ after $P2X_2$, $P2X_4$, $P2X_{2/6}$, or $P2X_{4/6}$ receptor activation (Figure 2C). For all four P2X receptors, inhibition of $I_{am\text{-}s}$ could not be achieved beyond approximately 90% inhibition, irrespective of any further increase in I_{ATP} charge transfer. The slope of the linear relationship for the $P2X_2$ receptor (0.8 ± 0.1, $n = 3$) and its heteromer (0.8 ± 0.2, $n = 3$) was less than that of the $P2X_4$ receptor (1.7 ± 0.2, $n = 3$) and its respective heteromer (1.7 ± 0.2, $n = 3$), suggesting different molecular mechanisms of I_{ATP}-induced $I_{am\text{-}s}$ inhibition.

$P2X_2$-Mediated Mechanism of $I_{am\text{-}s}$ *Inhibition*

Previous studies have demonstrated that an increase in intracellular Na^+ causes feedback inhibition of ENaC (5), thought to be triggered by the binding of Na^+ to a putative intracellular Na^+ receptor/binding site that is G protein linked and blocked by 5-N-dimethyl-amiloride (DMA) (28). In addition, it has been reported that P2 receptor–mediated activation of 4,4′-diisothiocyanostilbene-2,2′-disulfonic acid (DIDS)–sensitive calcium-activated Cl^- channels (CaCC), which are endogenous to *Xenopus* oocytes, results in the inhibition of $I_{am\text{-}s}$ (29). With these observations in mind, the molecular mechanism of P2X-mediated inhibition of $I_{am\text{-}s}$ was investigated pharmacologically.

We found that when $P2X_2$ receptors were coexpressed with ENaC and activated by 100 μM ATP (EC_{100}), decreasing the extracellular Na^+ concentration ($\Delta[Na^+]_{ext}$) from 100 to 80 mM led to a significant decrease (by 24 ± 4%, $n = 3$, $P < 0.05$) in the percentage inhibition of $I_{am\text{-}s}$ with no change in the amplitude of I_{ATP} (Figure 3A). Cytosolic injection of DMA (5 nl, 100 μM) into the oocyte 30 min before electrophysiologic recording completely abolished I_{ATP}-mediated inhibition of $I_{am\text{-}s}$ (96 ± 4% decrease in inhibition, $n = 3$, $P < 0.001$), with no change in the amplitude of I_{ATP}. Similarly, cytosolic injection of 50 μg/ml pertussis toxin (PTX), a G protein inhibitor, into the oocyte 24 h before recording also abolished the $P2X_2$-mediated inhibition of $I_{am\text{-}s}$ (97 ± 3% decrease in inhibition, $n = 3$, $P < 0.001$), with no change in the amplitude of I_{ATP}. Perfusion with 100 μM wortmannin, a phosphatidylinositol 3-kinase inhibitor, had the same effect (data not shown). Similar reductions in $I_{am\text{-}s}$ inhibition with $\Delta[Na^+]_{ext}$, DMA, and PTX were found for the $P2X_2$ heteromeric assembly $P2X_{2/6}$ (data not shown). However, applying 100 μM DIDS extracellularly, lowering extracellular concentrations of Cl^- acutely, incubating oocytes in low Cl^- for 72 h to reduce the cytosolic levels of Cl^- (low $[Cl^-]_{int}$), or

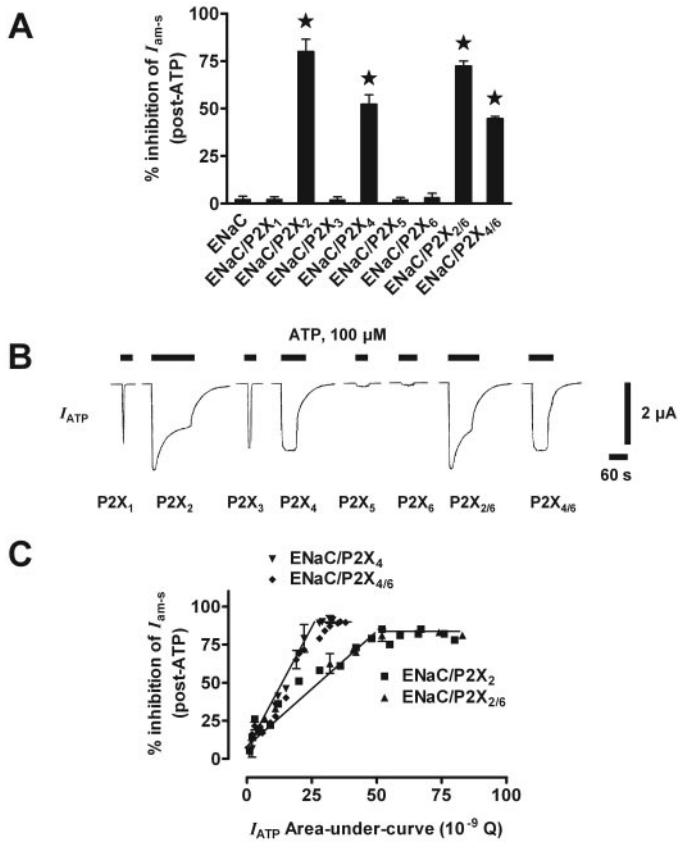

Figure 2. Selectivity of P2X-mediated inhibition of I_{am-s}. (A) Histogram comparing the percentage inhibition of I_{am-s} after activation of coexpressed P2X receptors by extracellular ATP (by an EC_{100} concentration of ATP). Data are expressed as a percentage of control I_{am-s} measured before activation of P2X receptors ($n = 3$). I_{am-s} was evoked by the removal of amiloride (10 μM) blockade at 20-min intervals. P2X receptors were activated 5 min before the subsequent I_{am-s} was evoked. (B) Typical P2X receptor–mediated currents evoked by 100 μM ATP ($V_h = -100$ mV). The largest and slowest desensitizing P2X-mediated currents correlated with the P2X receptors capable of inhibiting I_{am-s} (as shown in A). (C) The two distinct linear relationships between the percentage inhibition of I_{am-s} after the activation of $P2X_2$ (and $P2X_{2/6}$) and $P2X_4$ (and $P2X_{4/6}$) receptors by ATP (as shown in A; 5 min before the removal of 10 μM amiloride) *versus* the area under curve or charge transfer of P2X-mediated I_{ATP}. A range of ATP concentrations was used (100 nM to 100 μM), with each concentration of ATP repeated on at least three cells. For all four P2X receptors tested, inhibition of I_{am-s} could not be achieved beyond approximately 90% inhibition.

removing extracellular Ca^{2+} had no significant effect on the degree of $P2X_2$- or $P2X_{2/6}$-mediated inhibition of I_{am-s} (or the amplitude of I_{ATP}).

$P2X_4$-Mediated Mechanisms of I_{am-s} Inhibition

When $P2X_4$ receptors were coexpressed with ENaC and activated by 30 μM ATP (EC_{100}), changing $[Na^+]_{ext}$ from 100 to 80 mM resulted in a significant decrease (21 ± 2%, $n = 3$, $P < 0.05$) in the P2X-mediated inhibition of I_{am-s} (Figure 3B). In contrast to the $P2X_2$ and $P2X_{2/6}$ receptor experiments, DMA reduced

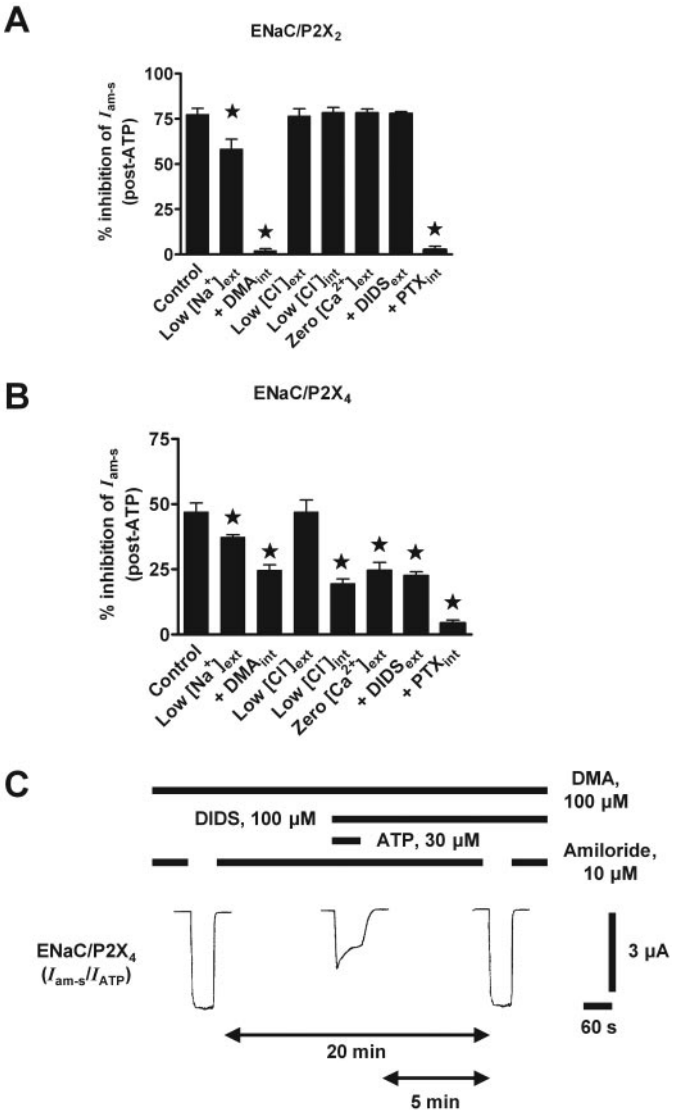

Figure 3. Mechanisms of P2X-mediated inhibition of ENaC currents. (A) Histogram showing the percentage inhibition of I_{am-s} as a result of ATP-evoked $P2X_2$ receptor activation, in a number of experimental conditions ($n = 3$ for each experimental condition). (B) As in A, histogram showing the effect of various experimental conditions on the percentage inhibition of I_{am-s} after P2X receptor activation, this time in oocytes that coexpressed ENaC and $P2X_4$ receptors ($n = 3$ for each condition). (C) A typical trace demonstrating that $P2X_4$-mediated inhibition of I_{am-s} is abolished in the presence of the calcium-activated Cl^- channel blocker 4,4′-diisothiocyanostilbene-2,2′-disulfonic acid (DIDS; 100 μM) and the injection of dimethyl amiloride (DMA; 100 μM) into oocytes 30 min before experimentation. PTX, pertussis toxin.

$P2X_4$-mediated inhibition by only 47 ± 6% ($n = 3$, $P < 0.01$). Acutely decreasing $[Cl^-]_{ext}$ had no effect, whereas incubation in low Cl^- for 72 h (low $[Cl^-]_{int}$), removal of $[Ca^{2+}]_{ext}$, or addition of the calcium-activated Cl^- channel blocker DIDS significantly reduced the inhibition of I_{am-s}, by 53 ± 8% ($n = 3$, $P < 0.01$), 45 ± 5% ($n = 3$, $P < 0.01$), and 47 ± 3% ($n = 3$, $P < 0.01$), respectively. As with $P2X_2$ and $P2X_{2/6}$, PTX abolished the

$P2X_4$-mediated inhibition of $I_{am\text{-}s}$ ($n = 3$). DIDS and zero extracellular Ca^{2+} (zero $[Ca^{2+}]_{ext}$) independently and additively reduced $P2X_4$-mediated inhibition of $I_{am\text{-}s}$ by approximately 50% without significantly altering the amplitude of I_{ATP} (data not shown). Given that DIDS, low $[Cl^-]_{int}$, and DMA independently reduced $P2X_4$-mediated inhibition of $I_{am\text{-}s}$ by approximately 50%, their effects were also tested additively. Figure 3C (a representative trace from $n = 3$) shows that the cytosolic injection of DMA (100 μM) and the perfusion of DIDS (100 μM) abolished $P2X_4$-mediated inhibition of $I_{am\text{-}s}$. Similarly, injection of DMA and incubation of oocytes in low Cl^- for 72 h (low $[Cl^-]_{int}$) also abolished the $P2X_4$-mediated inhibition of $I_{am\text{-}s}$. Furthermore, the application of DIDS to oocytes with low $[Cl^-]_{int}$ resulted in no further change in the reduction in inhibition of $I_{am\text{-}s}$. Collectively, these data suggest two independent mechanisms of inhibition: (*1*) an increase in $[Na^+]_{int}$ (as with the $P2X_2$ receptor) and (*2*) an increase in $[Ca^{2+}]_{int}$ leading to the activation of CaCC (and probable Cl^- efflux). Similar reductions in inhibitory effects on $I_{am\text{-}s}$ were observed with $\Delta[Na^+]_{ext}$, DMA, zero $[Ca^{2+}]_{ext}$, DIDS, DMA + DIDS, and PTX when using the $P2X_{4/6}$ receptor (data not shown).

Effect of Outward I_{ATP} *on* $I_{am\text{-}s}$

To confirm that inhibition of $I_{am\text{-}s}$ was due to an increase in intracellular Ca^{2+} and/or Na^+ carried by I_{ATP}, the V_h during application of ATP was increased from −100 to 50 mV, making I_{ATP} an outward current. $I_{am\text{-}s}$ was still recorded at −100 mV. For both $P2X_2$ and $P2X_4$ receptors, activation by a maximal concentration of ATP at V_h 50 mV had no significant effect on $I_{am\text{-}s}$ ($n = 3$). The area under the curve (and peak amplitude) for outward I_{ATP} ($V_h = 50$ mV) was $238 \pm 42 \times 10^{-10}$ Q (498 ± 72 nA) and $183 \pm 17 \times 10^{-10}$ Q (323 ± 89 nA) for $P2X_2$- and $P2X_4$-mediated currents, respectively (data not shown). Figure 2C confirms that the charge transfer of these outward currents, had they been inward currents, would have been sufficient to have inhibited $I_{am\text{-}s}$ significantly.

Time Course of P2X-Mediated Inhibition of $I_{am\text{-}s}$

For both $P2X_2$ and $P2X_4$ receptors, activation (and subsequent return to baseline, *i.e.*, deactivation of I_{ATP}) by extracellular ATP (100 and 30 μM, respectively), either immediately before or 5 min before the removal of amiloride, did not result in a significant change in the percentage inhibition of $I_{am\text{-}s}$ (immediately before 82 ± 6 and 52 ± 9% inhibition of $I_{am\text{-}s}$; 5 min before 80 ± 6 and 52 ± 5% inhibition of $I_{am\text{-}s}$, for $P2X_2$ and $P2X_4$ receptors, respectively), indicating that P2X-mediated inhibition of $I_{am\text{-}s}$ was immediate. Further analysis of the time course of P2X-mediated inhibition of $I_{am\text{-}s}$ by investigating the decay constant for I_{ATP} during the removal of amiloride blockade proved impossible because of the additive large whole-cell currents and the whole-cell voltage clamping limitations of the system.

Current/Voltage Relationships

Current/voltage (I/V) relationships for whole-cell currents were investigated for I_{ATP} and $I_{am\text{-}s}$. In oocytes in which ENaC was expressed alone, the I/V curve for $I_{am\text{-}s}$ showed inward rectification with a reversal potential (E_{rev}) of 10 ± 1 mV ($n = 3$; Figure 4A). Given an extracellular concentration of Na^+ of approximately 100 mM, the E_{rev} suggests partial Na^+ loading of the oocytes. Application of ATP (100 μM) did not change the I/V curve for $I_{am\text{-}s}$. I_{ATP} was negligible (<1 nA in amplitude) as expected, because *Xenopus* oocytes lack functional endogenous P2 receptors (30).

In oocytes that coexpressed ENaC and $P2X_2$ receptors, $I_{am\text{-}s}$ (before the activation of $P2X_2$ receptors) exhibited a similar inward rectification and E_{rev} to that found in oocytes that expressed ENaC alone ($E_{rev} = 10 \pm 2$ mV, $n = 3$; Figure 4B).

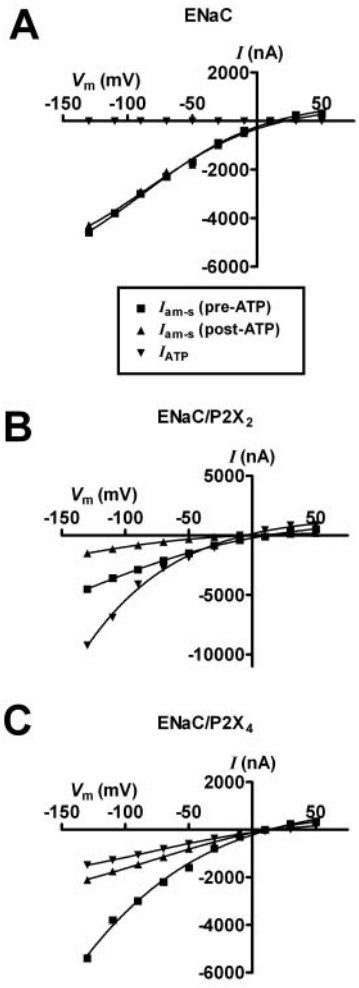

Figure 4. Average current/voltage (I/V) plots of amiloride-sensitive whole-cell currents ($I_{am\text{-}s}$) and ATP-sensitive whole-cell currents (I_{ATP}) measured in oocytes that expressed ENaC alone (A; $n = 3$) or coexpressed ENaC and $P2X_2$ receptors (B; $n = 3$) or ENaC and $P2X_4$ receptors (C; $n = 3$). Voltage pulse protocols were performed using step changes of the clamp potential from −90 to −130 mV up to 50 mV in 20-mV increments. $I_{am\text{-}s}$ was determined by subtracting the whole-cell current trace recorded in the presence of amiloride (10 μM) from that recorded in the absence of amiloride. $I_{am\text{-}s}$ was measured before ATP (100 μM) exposure (■) and 20 min later after ATP exposure (▲). I_{ATP} was measured during application of 100 μM ATP when I_{ATP} reached maximum amplitude (▼).

After an ATP challenge and activation of $P2X_2$ receptors, $I_{am\text{-}s}$ was found to be smaller in amplitude, yet the E_{rev} value (7 ± 2 mV, $n = 3$) and inward rectification were found to be unchanged. The 3-mV shift (NS) in the mean E_{rev} is compatible with a small change in the electrochemical Na^+ gradient as a result of an increase in intracellular Na^+. The I_{ATP} I/V curve showed inward rectification and an E_{rev} of −10 ± 1 mV ($n = 3$), as expected for either a poorly selective cation channel that conducts Na^+ and K^+ or one that conducts Cl^-. Because removal of extracellular Cl^- had no effect on $P2X_2$-mediated inhibition of $I_{am\text{-}s}$, the latter is unlikely (Figure 3A).

Figure 4C shows the I/V relationships for $I_{am\text{-}s}$ and I_{ATP} in oocytes that coexpressed ENaC and $P2X_4$ receptors. The curves for $I_{am\text{-}s}$, both before and after $P2X_4$ receptor activation, were inwardly rectifying with E_{rev} values of 10 ± 2 mV ($n = 3$) and 8 ± 2 mV ($n = 3$), respectively. After $P2X_4$ receptor activation, the amplitude of $I_{am\text{-}s}$ decreased. The $P2X_4$-mediated I_{ATP} I/V curve was inwardly rectifying with an E_{rev} value of 31 ± 4 mV ($n = 3$). This indicates a poorly selective cation channel permeable to Na^+ and Ca^{2+}, fitting with the pharmacologic findings shown in Figure 3B. Zero $[Ca^{2+}]_{ext}$ resulted in a negative shift of the E_{rev} to −8 ± 3 mV ($n = 3$), confirming that the $P2X_4$ receptor is additionally Ca^{2+} permeable (data not shown).

FLAG-Tagged ENaC: Receptor Trafficking

ENaC protein density in the plasma membrane was investigated using FLAG-tagged ENaC coexpressed with P2X receptors in *Xenopus* oocytes. Membrane chemiluminescence of bound anti-FLAG horseradish peroxidase–conjugated antibody was measured in intact oocytes before and after ATP exposure. Oocytes that expressed ENaC-FLAG and oocytes that coexpressed ENaC-FLAG and $P2X_2$ receptors showed chemiluminescence levels of 9.3 ± 2.0 ($n = 11$) and 7.1 ± 1.0 RLU ($n = 11$), respectively (NS). Addition of ATP (100 μM for 90 s) to oocytes that coexpressed ENaC and $P2X_2$ receptors resulted in a significant fourfold decrease in membrane chemiluminescence (1.7 ± 1.0 RLU, $n = 11$, $P < 0.01$; Figure 5). A similar decrease (3.5-fold) in membrane chemiluminescence ($n = 3$) was also measured in oocytes that coexpressed $P2X_4$ receptors and ENaC-FLAG after ATP exposure (data not shown). This suggests the removal of ENaC from the oocyte membrane after activation of the coexpressed $P2X_2$ and $P2X_4$ receptors by ATP.

The amplitude of $I_{am\text{-}s}$ in oocytes that expressed the FLAG-tagged ENaC subunits (ENaC-FLAG) was 3.9 ± 1.1 μA ($n = 10$ oocytes; $V_h = -100$ mV), which was not significantly different from that in oocytes that expressed nontagged ENaC subunits (3.7 ± 0.8 μA, $n = 50$ oocytes).

Maximum Current Amplitudes

During investigation of the effects of I_{ATP} on $I_{am\text{-}s}$, it became apparent that the maximal amplitude of $P2X_2$ receptor–mediated I_{ATP} was much greater (approximately 2.5-fold) when $P2X_2$ receptors were coexpressed with ENaC. We therefore investigated whether coexpression could affect the amplitude of maximal ENaC- or P2X receptor–mediated currents over a 5-d period (kept at 18°C) after the cytosolic injection of cRNA.

When ENaC was expressed alone, maximal $I_{am\text{-}s}$ was 3.5 ± 0.5 ($n = 3$), 3.7 ± 0.4 ($n = 3$), and 3.1 ± 0.2 μA at day 1, day 2, and day 3 after injection, respectively. $I_{am\text{-}s}$ decreased significantly by approximately 50% on day 5 to 1.2 ± 0.2 μA ($n = 3$, $P < 0.01$; Figure 6A), without affecting the slope of the inhibition curve or IC_{50} value for amiloride (data not shown). In contrast, when P2X receptors were expressed alone, maximal I_{ATP} remained relatively constant over the 5-d period (Figure 6B).

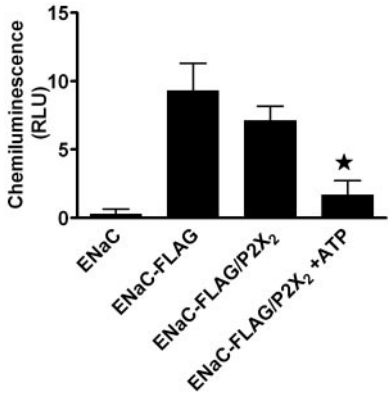

Figure 5. Activation of $P2X_2$ receptors by extracellular ATP decreases surface expression of ENaC-FLAG. A chemiluminescence assay was used to detect surface expression of extracellular FLAG-tagged ENaC in oocytes that expressed ENaC-FLAG alone or coexpressed $P2X_2$/ENaC-FLAG. Oocytes that expressed ENaC alone served as controls for nonspecific chemiluminescence. Single oocyte chemiluminescence was measured from 11 oocytes per group, and mean values are expressed in relative light units (RLU). FLAG sequence: DYKDDDDK.

Coexpression of ENaC with P2X receptors but the latter not activated did not significantly change the trend of maximal $I_{am\text{-}s}$ over the 5-d period (Figure 6C). Conversely, for certain P2X receptors that were coexpressed with ENaC but the latter blocked by amiloride (10 μM), the amplitude of I_{ATP} significantly increased over the first 3 d after injection. This increase in maximal I_{ATP} was evident for $P2X_2$ ($n = 3$), $P2X_{2/6}$ ($n = 3$), and $P2X_5$ ($n = 3$) receptors ($P < 0.01$ in each case; Figure 6, D and E). No change in the mean maximal amplitude of I_{ATP} was evident on day 4 or 5. Furthermore, no change in the ATP concentration-response curves or in the EC_{100} concentration was found (data not shown).

ENaC Coexpression Changes $P2X_2$ Membrane–Bound Protein Levels

Western blots using oocyte total membrane fractions were performed using a specific $P2X_2$ receptor antibody at days 1, 3, and 5 after ENaC and $P2X_2$ receptor cRNA injection to investigate whether there was an increase in $P2X_2$ receptor protein in oocytes that coexpressed ENaC. Figure 7A shows a representative Western blot. No band is evident for oocytes that expressed ENaC alone on days 1, 3, and 5, signifying that the $P2X_2$ receptor antibody did not cross-react with ENaC proteins. On days 1, 3, and 5, for oocytes that expressed $P2X_2$ receptors alone, a 56-kD protein band is seen. Comparison of these 56-kD bands with those observed for oocytes that coexpressed ENaC and $P2X_2$ receptors reveals a considerable increase in the den-

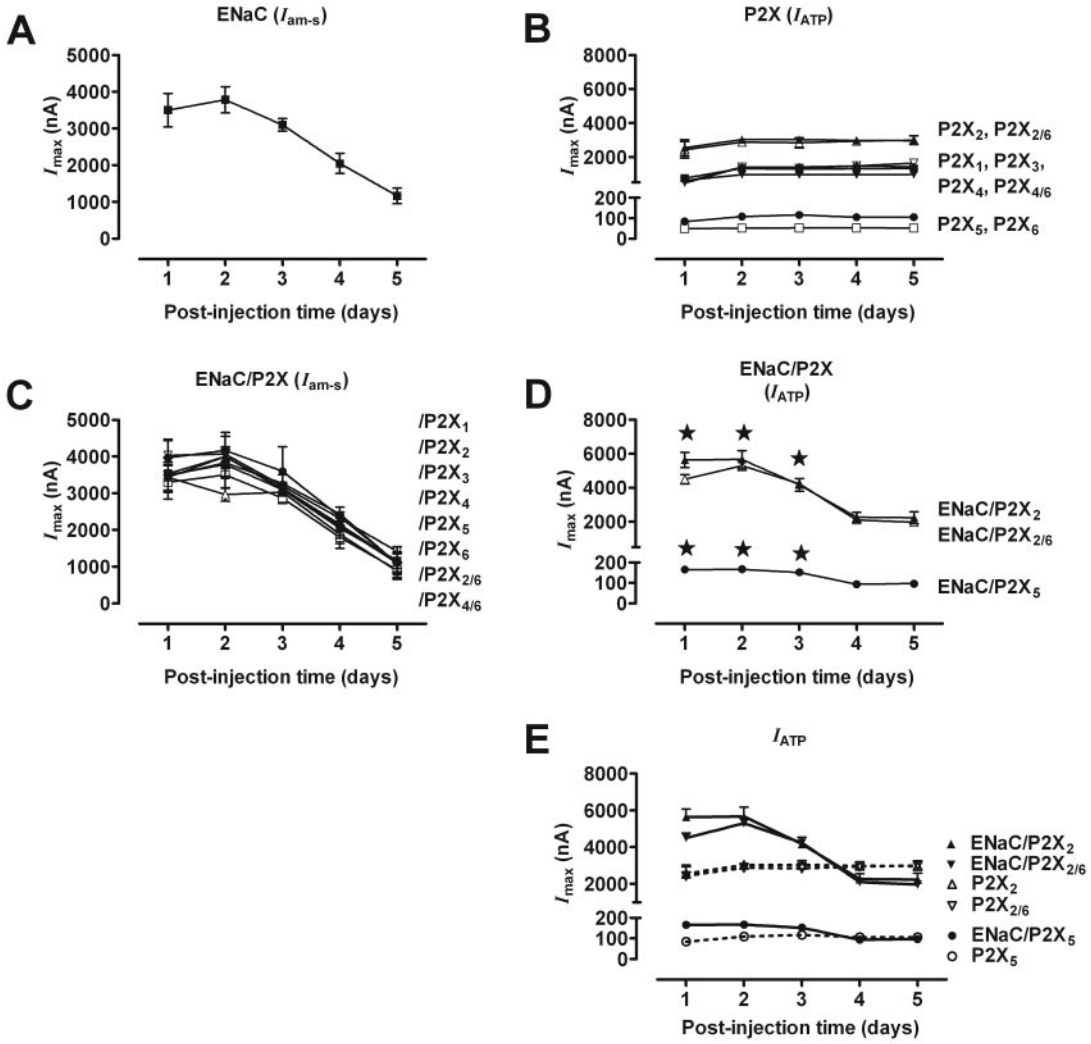

Figure 6. ENaC coexpression increases the maximum amplitude of I_{ATP}. (A) Amplitude of I_{am-s} evoked by the removal of amiloride (10 μM), in oocytes that expressed ENaC alone measured at 24-h intervals for 5 d after cRNA injection ($n = 3$ for each data point). (B) Amplitude of P2X-mediated currents evoked by a maximally stimulating concentration of ATP (I_{ATP}) in oocytes that expressed a series of P2X receptors alone, measured at 24-h intervals for 5 d after cRNA injection ($n = 3$ for each data point). (C) Amplitude of ENaC-mediated I_{am-s} in oocytes that coexpressed ENaC and members of a series of P2X receptors, measured at 24-h intervals for 5 d after cRNA injection ($n = 3$ in each case). Expressed P2X receptors were not activated. (D) Amplitude of maximal I_{ATP} in oocytes that coexpressed ENaC and P2X receptors whose maximal amplitude significantly altered in the presence of ENaC ($n = 3$ in each case). Coexpressed ENaC were blocked continuously by 10 μM amiloride. *$P < 0.01$. (E) Amplitude of maximal I_{ATP} in oocytes that coexpressed ENaC and P2X receptors whose maximal amplitude was significantly altered in the presence of ENaC compared with amplitude of maximal I_{ATP} in oocytes that expressed these P2X receptors alone (taken from B and D).

sity of the $P2X_2$ receptor band on days 1 and 3 but not 5. Band intensity was quantified and expressed as a percentage difference in $P2X_2$ protein intensity for oocytes that expressed $P2X_2$ alone and those that coexpressed ENaC/$P2X_2$. There were increases of 262 ± 136% ($n = 4$, $P < 0.01$) and 408 ± 275% ($n = 4$, $P < 0.01$) in $P2X_2$ protein intensity on days 1 and 3, respectively, whereas on day 5 there was no increase in intensity (Figure 7B).

ENaC coexpression may increase the expression of P2X receptors (and consequently the amplitude of maximal I_{ATP}) by increasing the delivery of receptor subunits to the cell surface or by inhibiting receptor retrieval. To assess the rate of retrieval (endocytosis), we inhibited delivery of new channels to the plasma membrane by incubating oocytes in 18 μM brefeldin A (BFA) for 4 h, 2 d after injection with cRNA. BFA significantly decreased maximal I_{ATP} amplitude for $P2X_2$ ($n = 3$), $P2X_{2/6}$ ($n = 3$), and $P2X_5$ ($n = 3$) receptors in the absence of ENaC by 57 ± 12 ($P < 0.01$), 61 ± 15 ($P < 0.01$), and 59 ± 17% ($P < 0.01$), respectively. In contrast, BFA did not alter I_{ATP} amplitude for $P2X_2$ ($n = 3$), $P2X_{2/6}$ ($n = 3$), and $P2X_5$ ($n = 3$) receptors in the presence of ENaC (by 9 ± 2%, 4 ± 5%, and 11 ± 7%, respectively). Given that BFA inhibits delivery of new P2X channels to the plasma membrane and that maximal I_{ATP} increases when $P2X_2$, $P2X_{2/6}$, and $P2X_5$ receptors are coexpressed with ENaC,

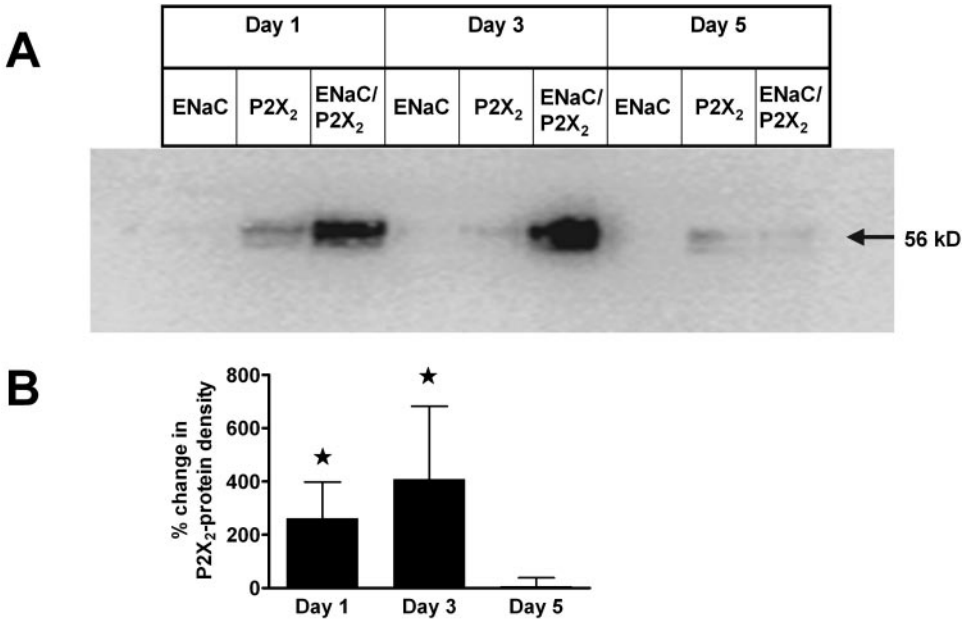

Figure 7. ENaC increase membrane expression of $P2X_2$ receptors. (A) Western blot analysis of $P2X_2$ receptor protein in oocyte membrane homogenates for oocytes that expressed ENaC alone (lane 1) and $P2X_2$ receptors alone (lane 2) and coexpressed ENaC/$P2X_2$ receptors (lane 3) at 1, 3, and 5 d after cRNA injection. (B) Density of western blot bands were quantified and expressed as the percentage difference in $P2X_2$ protein intensity for oocytes that expressed $P2X_2$ alone and those that coexpressed ENaC/$P2X_2$ ($n = 4$).

this suggests that the rate of P2X receptor retrieval is affected when ENaC and certain P2X receptors are coexpressed in *Xenopus* oocytes. When ENaC were expressed alone, BFA significantly decreased the amplitude of $I_{am\text{-}s}$ by 37 ± 9% ($n = 4$, $P < 0.05$); when ENaC were coexpressed with $P2X_2$, $P2X_{2/6}$, and $P2X_5$ receptors, BFA similarly decreased the amplitude of $I_{am\text{-}s}$ by 23 ± 7% ($n = 3$, $P < 0.05$), 32 ± 8% ($n = 3$, $P < 0.05$), and 34 ± 7% ($n = 3$, $P < 0.05$), respectively.

Discussion

It is known that the activity of ENaC in the distal nephron of the kidney is modified by the tubular perfusion of ATP or its analogues (19), even though ENaC itself is insensitive to extracellular ATP (17), and the mechanism of this inhibition is unresolved. In the present study, we have shown that activation of recombinant rat $P2X_2$, $P2X_4$, $P2X_{2/6}$, and $P2X_{4/6}$ receptor ion channels by extracellular ATP can inhibit amiloride-sensitive ENaC currents. This inhibition is due to a reduction in surface expression of ENaC, which is mediated by Na^+ influx and, in the case of $P2X_4$ and $P2X_{4/6}$ receptors, also by Ca^{2+} influx. Furthermore, we have shown that increasing expression levels of recombinant ENaC can result in a concomitant increase in coexpressed rat $P2X_2$, $P2X_{2/6}$, and $P2X_5$ receptors as a result of reduced retrieval from the plasma membrane (summarized in Figure 8).

Na^+-Dependent Mechanism of P2X Receptor–Mediated ENaC Downregulation

It was demonstrated previously that downregulation of ENaC occurs when $[Na^+]_{int}$ is increased during Na^+ reabsorption, an effect known as feedback inhibition (5,31). Although an increase in intracellular Na^+ is the trigger for ENaC downregulation, it has been demonstrated that this phenomenon is not mediated by a direct effect of Na^+ on the ENaC protein (5). Several cellular mechanisms have been proposed to explain feedback inhibition, of which the activation of the ubiquitin ligase Nedd4 seems particularly important (5,6,28,32,33). Hubner *et al.* (6) and Komwatana *et al.* (34) proposed that intracellular Na^+ binds initially to a putative Na^+ receptor, which, once activated, initiates a Nedd4-dependent signaling cascade involving G proteins and results in ubiquitination and retrieval of ENaC (34). In accordance with this proposed mechanism, we found that I_{ATP}-mediated inhibition of $I_{am\text{-}s}$ was completely abolished by DMA and by PTX. It therefore is plausible that the Nedd4 cascade plays a key role in the observed P2X-mediated inhibition of ENaC. Thus, P2X-mediated inhibition of ENaC may be achieved (entirely, in the case of $P2X_2$ and $P2X_{2/6}$, or partly, in the case of $P2X_4$ and $P2X_{4/6}$ receptors) *via* Na^+ feedback inhibition.

In previous studies, Na^+ feedback inhibition (in the absence of P2X receptor expression) was reported to occur at a much slower rate in *Xenopus* oocytes than we observed during P2X receptor stimulation (5,6). In both the present and previous studies, when ENaC (in the absence of amiloride) was exposed to high extracellular Na^+ concentrations (>100 mM), it took >25 min to achieve a 50% inhibition of ENaC-mediated Na^+ current ($V_h = -100$ mV) (7). In contrast, after $P2X_2$ and $P2X_{2/6}$ receptor activation, we found a rapid inhibition of $I_{am\text{-}s}$ (up to 90% within 5 min; Figure 2C). Thus, it seems that the influx of

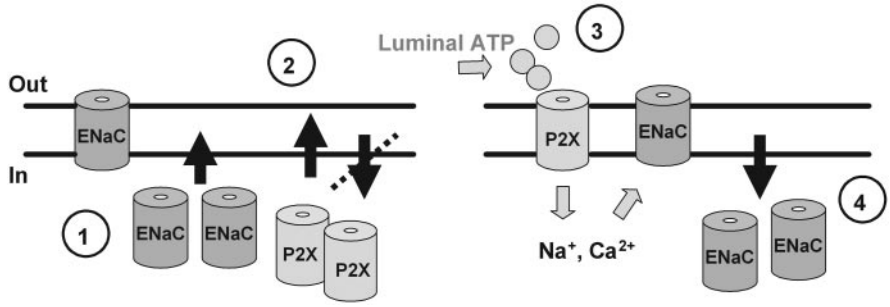

Figure 8. Potential regulatory interdependence of P2X receptors and ENaC. Schematic demonstrating that increased expression of ENaC (1) may result in the concomitant upregulation of $P2X_2$, $P2X_{2/6}$, and $P2X_5$ receptors (by decreased retrieval; 2). Activation of $P2X_2$, $P2X_4$, $P2X_{2/6}$, and/or $P2X_{4/6}$ receptor ion channels by endogenous extracellular ATP may result in an influx of Na^+ and Ca^{2+} (3) and the subsequent downregulation of ENaC (4).

Na^+ through $P2X_2$ and $P2X_{2/6}$ channels (and in part $P2X_4$ and $P2X_{4/6}$ channels) results in removal of ENaC from the plasma membrane at a much faster rate than does the influx of Na^+ through ENaC itself. Consequently, the mechanism by which P2X receptors inhibit ENaC is unlikely to be "classical" Na^+-mediated feedback inhibition. It is tempting to speculate that P2X receptor ion channels (or at least $P2X_2$, $P2X_4$, $P2X_{2/6}$, and $P2X_{4/6}$ receptors) may be in close proximity to ENaC, in such a way that activation of the P2X receptor results in a localized delivery of sodium ions to a site on or near ENaC that is particularly sensitive to increases in $[Na^+]_{int}$.

Ca^{2+}-Dependent Mechanism of P2X Receptor–Mediated ENaC Downregulation

A Ca^{2+}-dependent reduction in surface expression of ENaC was demonstrated previously in cultured epithelial cells in which downregulation of ENaC occurred after a P2Y receptor–mediated increase in $[Ca^{2+}]_{int}$ (14,20,35–37). However, this effect can be discounted in the present study because *Xenopus* oocytes are devoid of endogenous P2Y receptors (29). A study in cultured mIMCD-K2 cells (an immortalized mouse CD cell line in which $P2X_1$, $P2X_3$, and $P2X_4$ receptors are implicated in ENaC inhibition) is in keeping with our findings; this demonstrated Ca^{2+}-dependent inhibition of Na^+ reabsorption and stimulation of Cl^- secretion (after P2 receptor activation) (14,35). Also in accordance with our observations, downregulation of ENaC has been associated with the activation of apical CaCC in mouse endometrial epithelial cells (36). In the latter study, removal of extracellular Ca^{2+} or application of DIDS blocked inhibition of P2 receptor–mediated Na^+ absorption (and induction of Cl^- secretion). Evidence suggests that changes in cytosolic Cl^- concentration may mediate the inhibition of ENaC (31). However, to date, it remains controversial as to whether the inhibition of ENaC mediated by Cl^- currents (including CaCC currents) is (*1*) nonspecific and simply due to changes in intracellular Cl^- (31,38) or (*2*) specific to CFTR activation and the subsequent influx of Cl^- (39). The latter seems improbable given our recent recombinant findings. The exact mechanism by which activation of CaCC can result in the inhibition of ENaC or indeed the physiologic significance of Cl^- secretion-linked inhibition of ENaC has yet to be determined.

Mechanism of ENaC-Mediated P2X Receptor Upregulation

Our data demonstrate that an ENaC-mediated increase in $P2X_2$, $P2X_{2/6}$, and $P2X_5$ receptor whole-cell currents is due to an increase in P2X ion channel membrane expression. The number of ion channels expressed in the plasma membrane is determined by the balance between channel insertion into the membrane and retrieval from the plasma membrane. Our experiments using BFA (an inhibitor of channel delivery to the plasma membrane) demonstrate that the rate of P2X receptor *retrieval* is affected when ENaC is coexpressed with certain P2X receptors in *Xenopus* oocytes. This is in contrast to ENaC-mediated upregulation of ROMK1 (CFTR dependently) and CFTR, in which an increase in whole-cell currents in *Xenopus* oocytes was shown to be due to increased *insertion* into the plasma membrane (25). The ENaC-mediated increase in CFTR resulted in a two- to six-fold increase in cAMP-activated CFTR Cl^- currents, a magnitude not dissimilar to the increase that we observed for $P2X_2$ receptor currents. However, in the absence of single-channel data, we cannot discount the possibility that an increase in channel open probability could contribute to this effect, a possibility also raised in the ROMK1 and CFTR study (25).

The fact that only three specific P2X receptor subtypes were upregulated in response to increasing ENaC levels suggests that the P2X/ENaC interaction was specific and did not involve a nonspecific effect of ENaC on P2X protein degradation. It could be hypothesized that the mechanism of this linkage may involve a direct protein–protein interaction. There is already some evidence for direct physical interaction between P2X receptors and other ion channels. Intracellular cross-talk and physical interactions have been demonstrated between the $P2X_2$ receptor and the $5\text{-}HT_3$ serotonin-gated ion channel in myenteric neurons, *Xenopus* oocytes, and HEK293 cells (40), where concurrent activation of the ion channels produced non-additive currents and the channels co-immunoprecipitated and associated in clusters. Furthermore, in a recent study, it was demonstrated that activation of P2X receptors can lead to rapid cytoskeletal remodeling involving intracellular structural proteins (β-actin, α-actinin 4, laminin α3, and integrin β2) and membrane signaling proteins (phosphatidylinositol 4-kinase

and receptor protein tyrosine phosphatase β) (41). It is known that β-actin can directly regulate ENaC by modifying Ca^{2+}-dependent feedback inhibition (42). Consequently, protein–protein coupling may be responsible for the interactions between certain P2X receptors and ENaC.

Conclusion

In conclusion, these basic findings demonstrate a functional link between certain P2X receptor ion channels and ENaC. This interaction may provide an important mechanism for the coordinated regulation of Na^+ transport in epithelia that express P2X receptors, including the distal nephron of the kidney.

Acknowledgments

This work was supported by the Les Clark Fund; St. Peter's Trust for Kidney, Bladder and Prostate Research (UK); and the British Heart Foundation. S.S.W. is a recipient of a British Heart Foundation Research Fellowship.

Part of this study was presented at the American Society of Nephrology Renal Week, November 12 to 17, 2003, San Diego, CA (17,43) and the joint Experimental Biology and International Union of Physiologic Sciences meeting, March 31 to April 5, 2005, San Diego, CA (44).

We are grateful to Mary Rahman for molecular biology assistance; Dr. Chrystalla Orphanides for editorial assistance; Prof. Bernard Rossier for providing the three subunits of rat ENaC cDNA; Dr. Dmitri Firsov for providing three epitope-tagged subunits of rat ENaC cDNA; Dr. Gary Buell for providing rat $P2X_1$ cDNA; Dr. David Julius for providing rat $P2X_2$ cDNA; and Dr. Xuenong Bo and Prof. Alan North for providing rat $P2X_3$, $P2X_4$, $P2X_5$, and $P2X_6$ cDNA.

References

1. Schild L, Kellenberger S: Structure function relationships of ENaC and its role in sodium handling. *Adv Exp Med Biol* 502: 305–314, 2001
2. Hummler E, Horisberger J-D: Genetic disorders of membrane transport. The epithelial sodium channel and its implications in human diseases. *Am J Physiol* 276: G567–G571, 1999
3. Canessa CM, Schild L, Buell G, Thorens B, Gautschi I, Horisberger J, Rossier BC: Amiloride-sensitive epithelial Na+ channel is made of three homologous subunits. *Nature (Lond)* 367: 463–467, 1994
4. Garty H, Palmer LG: Epithelial sodium channels: Function, structure and regulation. *Physiol Rev* 77: 359–396, 1997
5. Abriel H, Horisberger J-D: Feedback inhibition of rat amiloride-sensitive epithelial sodium channels expressed in *Xenopus laevis* oocytes. *J Physiol (Lond)* 516: 31–43, 1999
6. Hubner M, Schreiber R, Boucherot A, Sanchez-Perez A, Poronnik P, Cook DI, Kunzelmann K: Feedback inhibition of epithelial Na+ channels in *Xenopus* oocytes does not require Go or Gi2 proteins. *FEBS Lett* 459: 443–447, 1999
7. Gormley K, Dong Y, Sagnella GA: Regulation of the epithelial sodium channel by accessory proteins. *Biochem J* 371: 1–14, 2003
8. Ralevic V, Burnstock G: Receptors for purines and pyrimidines. *Pharmacol Rev* 50: 413–492, 1998
9. North RA: Molecular physiology of P2X receptors. *Physiol Rev* 82: 1013–1067, 2002
10. Bo X, Jiang LH, Wilson HL, Kim M, Burnstock G, Suprenant A, North RA: Pharmacological and biophysical properties of the human P2X5 receptor. *Mol Pharmacol* 63: 1407–1416, 2003
11. Tsukimoto M, Harada H, Ikari A, Takagi K: Involvement of chloride in apoptotic cell death induced by activation of ATP-sensitive P2X7 purinoceptor. *J Biol Chem* 280: 2653–2658, 2005
12. Ruppelt A, Ma W, Borchardt K, Silberberg SD, Soto F: Genomic structure, developmental distribution and functional properties of the chicken P2X5 receptor. *J Neurochem* 77: 1256–1265, 2001
13. Turner CM, Vonend O, Chan C, Burnstock G, Unwin RJ: The pattern of distribution of selected ATP-sensitive P2 receptor subtypes in normal rat kidney: An immunohistological study. *Cells Tissues Organs* 175: 105–117, 2003
14. McCoy DE, Taylor AL, Kudlow BA, Karlson K, Slattery MJ, Schwiebert LM, Schwiebert EM, Stanton BA: Nucleotides regulate NaCl transport in mIMCD-K2 cells via P2X and P2Y purinergic receptors. *Am J Physiol Renal Physiol* 277: F552–F559, 1999
15. Taylor AL, Schwiebert LM, Smith JL, King C, Jones JR, Sorscher EJ, Schwiebert EM: Epithelial P2X purinergic receptor channel expression and function. *J Clin Invest* 104: 875–884, 1999
16. Unwin RJ, Bailey MA, Burnstock G: Purinergic signalling along the renal tubule: current state of play. *News Physiol Sci* 18: 237–241, 2003
17. Wildman SS, Chraibi A, Horisberger J-D, King BF, Unwin RJ: Downstream regulation of ENaC by ATP-gated P2X receptors. *J Am Soc Nephrol* 14: SA-FC165, 2003
18. Schwiebert EM, Zsembery A: Extracellular ATP as a signalling molecule for epithelial cells. *Biochim Biophys Acta* 1615: 7–32, 2003
19. Shirley DG, Bailey MA, Unwin RJ: In vivo stimulation of apical P2 receptors in collecting ducts: Evidence for inhibition of sodium reabsorption. *Am J Physiol Renal Physiol* 288: F1243–F1248, 2005
20. Lehrmann H, Thomas J, Kim SJ, Jacobi C, Leipziger J: Luminal P2Y2 receptor-mediated inhibition of Na+ absorption in isolated perfused mouse CCD. *J Am Soc Nephrol* 13: 10–18, 2002
21. Thomas J, Deetjen P, KO WH, Jacobi C, Leipziger J: P2Y(2) receptor-mediated inhibition of amiloride-sensitive short circuit current in M-1 mouse cortical collecting duct cells. *J Membr Biol* 183: 115–124, 2001
22. Ma H-P, Li L, Zhou ZH, Eaton DC, Warnock DG: ATP masks stretch activation of epithelial sodium channels in A6 distal nephron cells. *Am J Physiol Renal Physiol* 282: F501–F505, 2002
23. Leipziger J: Control of epithelial transport via luminal P2 receptors. *Am J Physiol Renal Physiol* 284: F419–F432, 2003
24. Wildman SS, Shirley DG, King BF, Unwin RJ: Indirect evidence for regulation of sodium reabsorption in sodium-restricted rats by an ATP-gated heteromeric P2X receptor. *J Physiol* 560P: PC11, 2004
25. Konstas AA, Koch JP, Tucker SJ, Korbmacher C: Cystic fibrosis transmembrane conductance regulator-dependent up-regulation of Kir1.1 (ROMK) renal K+ channels by the epithelial sodium channel. *J Biol Chem* 277: 25377–25384, 2002
26. Firsov D, Schild L, Gautschi I, Merillat A-M, Schneeberger E, Rossier BC: Cell surface expression of the epithelial Na chan-

nel and a mutant causing Liddle syndrome: A quantitative approach. *Proc Natl Acad Sci U S A* 93: 15370–15375, 1996
27. Bradford MM: A rapid and sensitive method for the quantitation of microgram quantities of protein utilizing the principle of protein-dye binding. *Anal Biochem* 72: 248–254, 1976
28. Komwatana P, Dinudom A, Young JA, Cook DI: Activators of epithelial Na+ channels inhibit cytosolic feedback control. Evidence for the existence of a G protein-coupled receptor for cytosolic Na+. *J Membr Biol* 162: 225–232, 1998
29. Cuffe JE, Bielfeld-Ackermann A, Thomas J, Leipziger J, Korbmacher C: ATP stimulates Cl− secretion and reduces amiloride-sensitive Na+ absorption in M-1 mouse cortical collecting duct cells. *J Physiol (Lond)* 524 1: 77–90, 2000
30. King BF, Wang S, Burnstock G: P2 purinoceptor activated inward currents in *Xenopus* oocytes. *J Physiol (Lond)* 494: 17–28, 1996
31. Turnheim K: Intrinsic regulation of apical sodium entry in epithelia. *Physiol Rev* 71: 429–445, 1991
32. Dinudom A, Young JA, Cook DI: Na+ and Cl− conductances are controlled by cytosolic Cl− concentration in the intralobular duct cells of mouse mandibular glands. *J Membr Biol* 135: 289–295, 1993
33. Abriel H, Loffing J, Rebhun JF, Pratt JH, Schild L, Horisberger JD, Rotin D, Staub O: Defective regulation of the epithelial Na+ channel by Nedd4 in Liddle's syndrome. *J Clin Invest* 103: 667–673, 1999
34. Komwatana P, Dinudom A, Young JA, Cook DI: Cytosolic Na+ controls the epithelial Na+ channel via the Go guanine nucleotide-binding regulatory protein. *Proc Natl Acad Sci U S A* 93: 8107–8111, 1996
35. Xia S-L, Wang L, Cash MN, Teng X, Schwalbe RA, Wingo CS: Extracellular ATP-induced calcium signalling in mIMCD-3 cells requires both P2X and P2Y purinoceptors. *Am J Physiol Renal Physiol* 287: F204–F214, 2004
36. Wang XF, Chan HC: Adenosine triphosphate induces inhibition of Na+ absorption in mouse endometrial epithelium: A Ca2+-dependent mechanism. *Biol Reprod* 63: 1918–1924, 2000
37. Kunzelmann K, Schrieber R, Boucherot A: Mechanisms of the inhibition of epithelial Na+ channels by CFTR and purinergic stimulation. *Kidney Int* 60: 455–461, 2001
38. Konig J, Schreiber R, Voelcker T, Mall M, Kunzelmann K: The cystic fibrosis transmembrane conductance regulator (CFTR) inhibits ENaC through an increase in the intracellular Cl− concentration. *EMBO Rep* 2: 1047–1051, 2001
39. Briel M, Gregor R, Kunzelmann K: Cl− transport by cystic fibrosis transmembrane conductance regulator (CFTR) contributes to the inhibition of epithelial Na+ channels (ENaCs) in *Xenopus* oocytes co-expressing CFTR and ENaC. *J Physiol* 508: 825–836, 1998
40. Boue-Grabot E, Barajas-Lopez C, Chakfe Y, Blais D, Belanger D, Emerit MB, Seguela P: Intracellular cross talk and physical interactions between two classes of neurotransmitter-gated channels. *J Neurosci* 23: 1246–1253, 2003
41. Kim M, Jiang LH, Wilson HL, North RA, Surprenant A: Proteomic and functional evidence for a P2X7 receptor signalling complex. *EMBO J* 20: 6347–6358, 2001
42. Berdiev BK, Latorre R, Benos DJ, Ismailov II: Actin modifies Ca2+ block of epithelial Na+ channels in planar lipid bilayers. *Biophys J* 80: 2176–2186, 2001
43. Wildman SS, Chraibi A, Horisberger J-D, King BF, Unwin RJ: Does ENaC regulate membrane trafficking of other ion channels? *J Am Soc Nephrol* 14:SA-FC169, 2003
44. Wildman SS, Marks J, Churchill LJ, Peppiatt CM, Horisberger J-D, King BF, Unwin RJ: Molecular cross-talk between cloned epithelial sodium channels and ATP-gated P2X receptors. *FASEB J* 19: A1177, 2005